UDC 539.3

Z. Zhuravlova[1], D. Nerukh[2], V. Reut[1], N. Vaysfel'd[1]

INVESTIGATION OF IDEALIZED VIRUS CAPSID MODEL WITH THE DYNAMIC ELASTICITY APPARATUS

The three-dimensional dynamic theory of elasticity is applied to investigate the mechanical properties of virus capsid. The idealized model of the virus is based on the 3D boundary-value problem of mathematical physics formulated in spherical coordinate system for the steady-state oscillation process. The virus is modeled as a hollow elastic sphere filled by acoustic medium and is located in different acoustic medium. The stated boundary-value problem is solved with the help of the integral transform method and method of the discontinuous solutions. As a result, the exact solution of the problem is obtained. The numerical calculations of the virus elastic characteristics are carried out.

The development of virus mathematical model is necessary to representing the effect of parameters variation on the behavior of a virus as a dynamic system. Such mathematical models based on the reasonable biological assumptions were obtained earlier within three main interdisciplinary approaches: ***1***) the hydrodynamic approach [23, 21, 30]; ***2***) the approach with the use of the numerical methods for solving the nonlinear problems of hydrodynamics and elasticity [16, 18, 28, 29, 36]; ***3***) the approach based on the linear elasticity models [15, 34, 36]. The mentioned models allowed to obtain many important characteristics of the virus, but they could not fully solve the problem of investigation of the virus as a 3D elastic object. In this paper the authors first propose to use the complete system of motion equations of linear elasticity for representation of virus wave field. It allows to take into consideration the virus 3D structure and to obtain its new qualitative characteristics.

The morphology of icosahedral viruses ranges from highly spherical to highly faceted, and for some viruses a shape transition occurs during the viral life cycle. This phenomena is predicted from continuum elasticity, via the buckling transition theory by Nelson [22], in which the shape is dependent on the Foppl – von Karman number γ, which is a ratio of the two-dimensional Young's modulus, Y, and the bending modulus $æ$: $\gamma = YR^2/æ$ (R is the virus radius). However, until now, no direct calculations have been performed on atomic-level capsid structures to test the predictions of the theory.

The elasticity and mechanical stability of empty and filled viral capsids under external force loading are studied in a combined analytical and numerical approach. Quantitative measurements of the mechanical response of nanosized protein shells (viral capsids) to large-scale physical deformations were reported in [29]. These measurements were compared with theoretical descriptions from continuum modeling and molecular dynamics. In [22] it was shown that the icosahedral packings of protein capsomeres proposed by Caspar and Klug for spherical viruses become unstable to faceting for sufficiently large virus size. A model, based on the nonlinear physics of thin elastic shells, produced excellent one-parameter fits in real space to the full three-dimensional shape of large spherical viruses. The mechanical properties of individual empty capsid and DNA-containing virions of the minute virus of mice were investigated by using atomic force microscopy in [17]. The stiffness of the empty capsid was found to be isotropic. Remarkably, the presence of DNA inside the virion leads to an anisotropic reinforcement of the virus stiffness by $\approx 3\,\%$, 40 %, and 140 % along the fivefold, threefold, and twofold symmetry axes respectively. An emerging paradigm for self-organized soft materials, geometrically frustrated assemblies, where interactions between self-assembling elements (e.g., particles, macromolecules, proteins) favor local

packing motifs that are incompatible with uniform global order in the assembly was overviewed in [19]. Some of the key ideas that have been set in both the materials and biological settings were described in general terms in [27]. Some future developments along these lines were speculated. An atomistic force-probe molecular dynamics simulations of the complete shell of southern bean mosaic virus, a prototypical $T = 3$ virus, was performed in explicit solvent in [36]. It was done to study the distribution and heterogeneity on the virus surface of the mechanical properties of viral shells. A course-grained modeling approach within the framework of three-dimensional nonlinear continuum elasticity was adopted in [18]. Homogeneous, isotropic, elastic, thick-shell models were proposed for two capsids: the spherical cowpea chlorotic mottle virus, and the ellipsocylindrical bacteriophage $\varphi 29$. The mechanical properties of crystalline shells of icosahedral symmetry on a substrate under a uniaxial applied force were studies in [32] by computer simulations. The elastic response for small deformations, and the buckling transitions at large deformations were predicted. A previously described multiscale method by May and Brooks was employed to calculate Y and $æ$ for the bacteriophage HK97 in [24], which undergoes a spherical to faceted transition during its viral life cycle. A change in γ consistent with the buckling transition theory was observed and a significant reduction in $æ$, which facilitates formation of the faceted state, was studied. The influence of capsid structure and chirality on the mechanical properties were analyzed in [15]. It was found that generally skew shells have lower stretching energy. The mechanical properties of viral capsids, calling explicit attention to the inhomogeneity of the shells that is inherent to their discrete and polyhedral nature, were investigated in [34]. The distribution of stress in these capsids was calculated, and their response to isotropic internal pressure was analyzed.

Static-state fluctuations in three-dimensional bodies were studied in many works (see, e.g., [2, 5, 7, 8, 10, 25]) in view of the necessity of their practical engineering applications.

Several problems for hollow spheres were investigated by many authors. It should be pointed the classical works by Grinchenko and Meleshko [3], Ulitko [9], Chernina [12].

The transient response of the fluid-shell system of a thin, elastic and ring-stiffened spherical shells, which accelerates in an acoustic medium was studied numerically in [13]. The problem of scattering of a plane sound wave by an acoustically rigid spherical shell with spherical inclusion in the unlimited homogeneous isotropic media [20] was reduced to solving dual series equations on Legendre polynomials. The dual equations were transformed into an infinite system of linear algebraic equations of the second kind with a completely continuous operator. The motion of a rigid sphere in a viscoelastic medium in response to an acoustic radiation force of short duration was investigated in [14]. The multiple scattering of a spherical acoustic wave from an arbitrary number of fluid spheres was investigated theoretically in [33]. A problem on radial oscillations of the hollow elastic inhomogeneous transverse-isotropic sphere in unlimited acoustic medium was investigated in [6]. The theory of resonance scattering was used in [11] for solving the problem of sound scattering from an elastic transversely isotropic solid sphere in an ideal acoustic fluid medium. The solution is obtained with use the normal mode expansion technique in conjunction with the Frobenius power series.

As it is seen from the literature analysis the apparatus of 3D elasticity can be efficiently applied for the constuction of the idealized capsid model.

1. The statement of the problem. A porcine circovirus type 2 (PCV2) (see Fig. 1) is modeled by a hollow elastic sphere occupying the area $R_1 < r < R_2$, $0 < \theta < 2\pi$, $-\pi < \varphi < \pi$ in the spherical coordinate system.

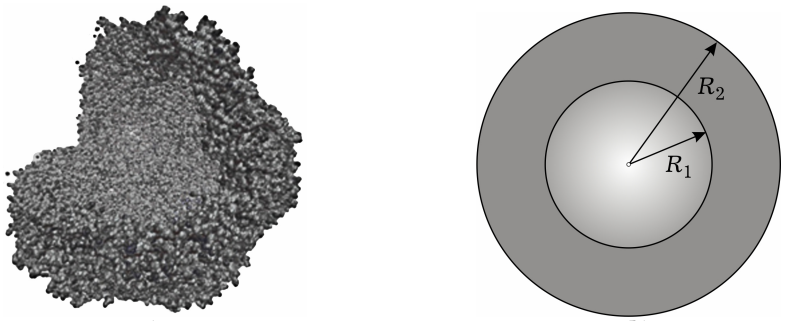

a) ***b***)

Fig. 1. The geometry of idealized capsid model: ***a***) – PCV2 at full atom resolution; ***b***) – the mathematical model of the virus.

Motion equations are written with respect to the displacements $u = u_r(r,\theta,\varphi,t)$, $v = u_\theta(r,\theta,\varphi,t)$, $w = u_\varphi(r,\theta,\varphi,t)$ in the following form [26]:

$$\nabla^2 u_r - \frac{2}{r^2}\left[u_r + \frac{1}{\sin\theta}\frac{\partial}{\partial\theta}(u_\theta \sin\theta) + \frac{1}{\sin\theta}\frac{\partial u_\varphi}{\partial\varphi}\right] + \\ + \tilde{\lambda}\frac{\partial}{\partial r}H(u_r,u_\theta,u_\varphi,r,\theta,\varphi) = \tilde{\rho}\frac{\partial^2 u_r}{\partial t^2},$$

$$\nabla^2 u_\theta + \frac{2}{r^2}\left[\frac{\partial u_r}{\partial\theta} - \frac{1}{2\sin^2\theta}u_\theta - \frac{\cos\theta}{\sin^2\theta}\frac{\partial u_\varphi}{\partial\varphi}\right] + \\ + \tilde{\lambda}\frac{1}{r}\frac{\partial}{\partial\theta}H(u_r,u_\theta,u_\varphi,r,\theta,\varphi) = \tilde{\rho}\frac{\partial^2 u_\theta}{\partial t^2},$$

$$\nabla^2 u_\varphi + \frac{2}{r^2\sin\theta}\left[\frac{\partial u_r}{\partial\varphi} + \operatorname{ctg}\theta\frac{\partial u_\theta}{\partial\varphi} - \frac{u_\varphi}{2\sin\theta}\right] + \\ + \frac{\tilde{\lambda}}{r\sin\theta}\frac{\partial}{\partial\varphi}H(u_r,u_\theta,u_\varphi,r,\theta,\varphi) = \tilde{\rho}\frac{\partial^2 u_\varphi}{\partial t^2}, \qquad (1)$$

where

$$\nabla^2 = \frac{1}{r^2}\frac{\partial}{\partial r}\left(r^2\frac{\partial}{\partial r}\right) + \frac{1}{r^2\sin\theta}\frac{\partial}{\partial\theta}\left(\sin\theta\frac{\partial}{\partial\theta}\right) + \frac{1}{r^2\sin\theta}\frac{\partial^2}{\partial\varphi^2},$$

$$H(u_r,u_\theta,u_\varphi,r,\theta,\varphi) = \frac{1}{r^2}\frac{\partial}{\partial r}(r^2 u_r) + \frac{1}{r\sin\theta}\frac{\partial}{\partial\theta}(u_\theta\sin\theta) + \frac{1}{r\sin\theta}\frac{\partial u_\varphi}{\partial\varphi},$$

ν is Poisson's ratio, E is Young's modulus, $\mu = \dfrac{E}{2(1+\nu)}$, $\lambda = \dfrac{\nu E}{(1+\nu)(1-2\nu)}$,

$\tilde{\lambda} = \dfrac{\lambda+\mu}{\mu}$, ρ is virus density, $\tilde{\rho} = \dfrac{r^2\rho}{\mu}$.

It is assumed that the virus is filled and surrounded with two dissimilar acoustic media. The wave potentials $\Phi_i(r,\theta,\varphi,t)$ of the external, $i=2$, and the internal, $i=1$, acoustic media satisfy the wave equations [4]

$$\Delta\Phi_i = \frac{1}{c_i^2}\frac{\partial^2\Phi_i}{\partial t^2}, \qquad t>0, \qquad i=1,2, \qquad (2)$$

here c_i, $i=1,2$, are wave velocities.

It is assumed that adhesion occurs on the contact surfaces of virus and surrounding acoustic media

$$\sigma_r(R_1+0,\theta,\varphi,t) = -p_1(\theta,\varphi,t)\big|_{r=R_1} = \rho_1\frac{\partial}{\partial t}\Phi_1(R_1-0,\theta,\varphi,t),$$

$$\sigma_r(R_2-0,\theta,\varphi,t) = -p_2(\theta,\varphi,t)\big|_{r=R_2} = \rho_2\frac{\partial}{\partial t}(\Phi_2+\Phi_0)(R_2+0,\theta,\varphi,t), \qquad (3)$$

$$\tau_{r\varphi}\big|_{r=R_i} = \tau_{r\theta}\big|_{r=R_i} = 0, \qquad i = 1,2. \tag{4}$$

It is also assumed that on the contact surfaces of virus and surrounding acoustic media the such conditions for velocities are satisfied:

$$\frac{\partial u_r}{\partial t}(R_1 + 0, \theta, \varphi, t) = \frac{\partial \Phi_1}{\partial r}(R_1 - 0, \theta, \varphi, t),$$
$$\frac{\partial u_r}{\partial t}(R_2 - 0, \theta, \varphi, t) = \frac{\partial}{\partial r}(\Phi_2 + \Phi_0)(R_2 + 0, \theta, \varphi, t). \tag{5}$$

The boundary conditions with respect to the variables θ and φ can be formulated as displacements or stresses which are given on the surfaces. Here it was proposed that the conditions of the second main elasticity problem are fulfilled.

One has to determine the wave field under the influence of a spherical pressure wave $\Phi_0(r, \theta, \varphi, t)$ which incident on the virus external surface and satisfies Zommerfeld's conditions.

2. The reformulation of the stated problem in the form of the discontinuous boundary problem. The steady-state oscillations are considered:

$$u_r(r, \theta, \varphi, t) = u(r, \theta, \varphi)e^{i\omega_0 t}, \qquad u_\theta(r, \theta, \varphi, t) = v(r, \theta, \varphi)e^{i\omega_0 t},$$
$$u_\varphi(r, \theta, \varphi, t) = w(r, \theta, \varphi)e^{i\omega_0 t},$$
$$\Phi_j(r, \theta, \varphi, t) = \tilde{\Phi}_j(r, \theta, \varphi)e^{i\omega_j t}, \qquad j = 1,2, \tag{6}$$

here ω_0, ω_1, ω_2 are oscillation frequencies of the sphere, internal and external acoustic environments, respectively.

The tilde symbol in $\tilde{\Phi}_j(r, \theta, \varphi)$ will be omitted from now on.

The finite Fourier transform method is applied to equations (1), (2) and boundary conditions (3)–(5) with regard to variable φ [31].

The transformations of the unknown functions are presented as a superposition of the functions $u_n = u_n^1 + u_n^2$, $v_n = v_n^1 + v_n^2$, $w_n = w_n^1 + w_n^2$, where the upper index «1» denotes the mechanical characteristics, which are discontinuous on the interior surface of the spherical shell, and the upper index «2» denotes the mechanical characteristics, which are discontinuous on the external surface of the spherical shell [35]

$$\langle f_n \rangle\big|_{r=R_1} = \langle f_n^1 \rangle\big|_{r=R_1} + \langle f_n^2 \rangle\big|_{r=R_1} = \langle f_n^1 \rangle\big|_{r=R_1} = -f_n^1(R_1 + 0, \theta),$$
$$\langle f_n \rangle\big|_{r=R_2} = \langle f_n^1 \rangle\big|_{r=R_2} + \langle f_n^2 \rangle\big|_{r=R_2} = \langle f_n^2 \rangle\big|_{r=R_2} = f_n^2(R_2 - 0, \theta), \tag{7}$$

where $\langle f_n \rangle\big|_{r=R_i} = f_n(R_i - 0, \theta) - f_n(R_i + 0, \theta)$, $f \in \{u, v, w, \sigma_r, \tau_{r\theta}, \tau_{r\varphi}\}$. For the external wave field the wave potential is constructed as a superposition of the field generated by the incident wave and the wave scattered on the external shell of the virus:

$$\Phi_{2n}(r, \theta) = \Phi_{2n}(r, \theta) + \Phi_{0n}(r, \theta).$$

The jumps of the acoustic potentials are introduced in the following way. Since acoustic environments are inside and outside the spherical shell,

$$\Phi_{1n}(r, \theta) = 0, \quad r > R_1, \qquad \Phi_{2n}(r, \theta) = 0, \quad r < R_2,$$

and

$$\langle \Phi_{1n} \rangle\big|_{r=R_1} = \Phi_{1n}(R_1 - 0, \theta) - \Phi_{1n}(R_1 + 0, \theta) = \Phi_{1n}(R_1 - 0, \theta),$$
$$\langle \Phi_{2n} \rangle\big|_{r=R_2} = \Phi_{2n}(R_2 - 0, \theta) - \Phi_{2n}(R_2 + 0, \theta) + \Phi_{0n}(R_2, \theta) =$$
$$= -\Phi_{2n}(R_2 + 0, \theta) + \Phi_{0n}(R_2, \theta). \tag{8}$$

Conditions (3) and (5) can be rewritten with regard to the formulas (7) and (8) as

$$\sigma_r^1(R_2-0,\theta,\varphi,t)+\sigma_r^2(R_2-0,\theta,\varphi,t)=\rho_2\frac{\partial}{\partial t}(\Phi_2+\Phi_0)(R_2+0,\theta,\varphi,t),$$

$$\sigma_r^1(R_1+0,\theta,\varphi,t)+\sigma_r^2(R_1+0,\theta,\varphi,t)=\rho_1\frac{\partial}{\partial t}\Phi_1(R_1-0,\theta,\varphi,t), \qquad (9)$$

$$\frac{\partial u_r^1}{\partial t}(R_1+0,\theta,\varphi,t)+\frac{\partial u_r^2}{\partial t}(R_1+0,\theta,\varphi,t)=\frac{\partial}{\partial r}\Phi_1(R_1-0,\theta,\varphi,t),$$

$$\frac{\partial u_r^1}{\partial t}(R_2-0,\theta,\varphi,t)+\frac{\partial u_r^2}{\partial t}(R_2-0,\theta,\varphi,t)=\frac{\partial}{\partial r}(\Phi_2+\Phi_0)(R_2+0,\theta,\varphi,t). \qquad (10)$$

Accordingly to [1] the discontinuous solution for a spherical defect in the finite Fourier transform domain has the form shown in ***Appendix A.*** It depends on unknown jumps of displacements $\left\langle u_{nk}^i(R_i)\right\rangle$ and unknown jumps of stresses $\left\langle \sigma_{rnk}^i(R_i)\right\rangle$, $i=1,2$.

The Legendre integral transform is applied with respect to variable θ by the rule

$$f_{nk}(r)=\int_0^\pi \sin\theta\, P_k^{|n|}(\cos\theta) f_n(r,\theta)\, d\theta,$$

where $f\in\{u^i,v^i,w^i,\sigma_r^i,\tau_{r\theta}^i,\tau_{r\varphi}^i,\Phi_j^i\}$, $i,j=1,2$, with the inverse formulas

$$f_n(r,\theta)=\sum_{k=|n|}^{\infty} f_{nk}(r)\,\sigma_{k,|n|}\,P_k^{|n|}(\cos\theta),$$

here $\sigma_{k,|n|}=\dfrac{(k-|n|)!(k+1/2)}{(k+|n|)!}$.

The discontinuous solution for the acoustic potentials in the transform domain has the following form:

$$\Phi_{ink}(r)=R_i^2\left[\left\langle\Phi'_{ink}(R_i)\right\rangle\Gamma_{ik}(r,R_i)-\left\langle\Phi_{ink}(R_i)\right\rangle\frac{\partial}{\partial R_i}\Gamma_{ik}(r,R_i)\right],\ i=1,2, \qquad (11)$$

where

$$\Gamma_{i,k}(r,R_j)=\frac{\pi i}{2\sqrt{rR_j}}\begin{cases}I_\nu(R_jq_i)K_\nu(rq_i), & r>R_j,\\ I_\nu(rq_i)K_\nu(R_jq_i), & r<R_j,\end{cases}\quad k=0,1,2,\ldots,\ \nu=k+1/2,$$

$$q_j^2=-\frac{\omega_j^2}{c_j^2},\qquad j=1,2.$$

3. Derivation of the calculation formulas describing the wave field. To get the calculation formulas one has to determine the wave potentials jumps and its derivatives, and also the displacement and stress jumps.

In view of the formulas (8) one can obtain the correlations between the jumps in the transform domain:

$$\left\langle\Phi'_{1nk}(R_i)\right\rangle=\left\langle\Phi_{1nk}(R_1)\right\rangle g_{1k}(R_1),$$

$$\left\langle\Phi'_{2nk}(R_i)\right\rangle=\left\langle\Phi_{2nk}(R_2)\right\rangle g_{2k}(R_2),$$

where

$$g_{1k}(R_1)=\frac{\frac{\partial}{\partial R_1}\Gamma_{1k}(R_1+0,R_1)}{\Gamma_{1k}(R_1+0,R_1)},\qquad g_{2k}(R_2)=\frac{\frac{\partial}{\partial R_2}\Gamma_{2k}(R_2-0,R_2)}{\Gamma_{2k}(R_2-0,R_2)},$$

Thus

$$\Phi_{ink}(r) = R_i^2 \left\langle \Phi_{ink}(R_i) \right\rangle \left[g_{ik}(R_i) - \frac{\partial}{\partial R_i} \Gamma_{ik}(r, R_i) \right], \quad i = 1,2. \tag{12}$$

To determine jumps $\left\langle u_{nk}^i(R_i) \right\rangle$, $\left\langle \sigma_{rnk}^i(R_i) \right\rangle$, $i = 1,2$, the conditions (3), (5) are used. So one can obtain formulas for jumps $\left\langle u_{nk}^i(R_i) \right\rangle$, $\left\langle \sigma_{rnk}^i(R_i) \right\rangle$, $i = 1,2$, depending on acoustic potential jumps:

$$\left\langle \sigma_{rsnk}^1(R_1) \right\rangle = -\rho_1 s_1 (\Phi_{0snk}^1 + \Phi_{1snk}) \Big|_{r=R_1-0} = -\rho_1 s_1 \Big(\Phi_{0snk}^1 + \\ + R_1^2 \left\langle \Phi_{1nk}(R_1) \right\rangle \left[g_{1k}(R_1) - \frac{\partial}{\partial R_1} \Gamma_{1k}(r, R_1) \right] \Big) \Big|_{r=R_1-0},$$

$$\left\langle \sigma_{rsnk}^2(R_2) \right\rangle = \rho_2 s_2 (\Phi_{0snk}^2 + \Phi_{2snk}) \Big|_{r=R_2+0} = \rho_2 s_2 \Big(\Phi_{0snk}^2 + \\ + R_2^2 \left\langle \Phi_{2nk}(R_2) \right\rangle \left[g_{2k}(R_2) - \frac{\partial}{\partial R_2} \Gamma_{2k}(r, R_2) \right] \Big) \Big|_{r=R_2+0},$$

where $\Phi_{01snk}(R_1)$, $\Phi_{02snk}(R_2)$ are transforms of the incident waves from the inner and outer acoustic environments, respectively.

To determine jumps $\left\langle \Phi_{ink}(R_i) \right\rangle$, $i = 1,2$, the second condition in (4) is used. So one can get the system of two complex linear equations for $\left\langle \Phi_{ink}(R_i) \right\rangle$, $i = 1,2$.

After inversing the Fourier transform by the formulas (7) and taking into account the steady-state oscillations (5) one can obtain the final formulas for the displacements.

4. Discussion. The calculations were done for the elastic thick shell ($E = 0.25 \cdot 10^9$ Pa, $\mu = 0.4$, $\rho = 750$ a.u./nm^3) with the inner and outer radiuses $R_1 = 10.4 \cdot 10^{-9}$ m, $R_2 = 13.2 \cdot 10^{-9}$ m, respectively. The values of the speed of sound for internal and external acoustic environments are $c_1 = 1400$ m/s (water), $c_2 = 1560$ m/s (sea water), respectively.

Consider the case when frequencies of spherical shell, inner and outer acoustic environments are $\omega_0 = 0.1$, $\omega_1 = 0.1$, $\omega_2 = 0.2$, incident waves from the inner and outer acoustic environments are

$$\Phi_{01}(R_1, \theta, \varphi, t) = 0,$$

$$\Phi_{02}(R_2, \theta, \varphi, t) = \begin{cases} \dfrac{e^{i(kR_2 - \omega_2 t)}}{R_2} 10^{-42}, & \dfrac{\pi}{4} \le \theta \le \dfrac{\pi}{2}, \\ 0, & 0 < \theta < \dfrac{\pi}{4}, \dfrac{\pi}{2} < \theta < \pi, \end{cases} \qquad k = \frac{\omega_2}{c_2}.$$

In Fig. 2 the dependence of the displacements u_r at the inner and outer surfaces of the spherical shell on θ is presented. When θ changes from 0 to π, displacements u_r increase. As can be seen, maximal spikes at the inner surface ($r = R_1$) are larger than at the outer surface ($r = R_2$). The dependence of the displacements u_θ at the inner and outer surfaces of the spherical shell on θ is shown in Fig. 3 . The periodicity of the displacements u_θ is observed. As can be seen, the displacements u_θ on the outer surface ($r = R_2$) are larger than displacements at the inner surface ($r = R_1$). Values of the displacements u_θ are obviously less than displacements u_r values.

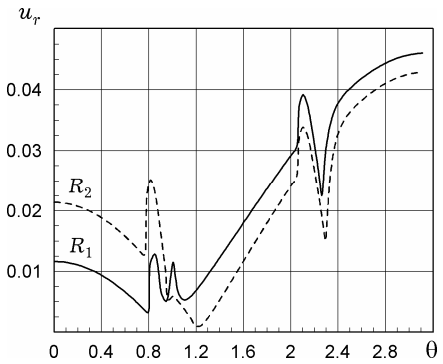

Fig. 2. Dependence of the displacements u_r at the inner and outer surfaces of the spherical shell on θ.

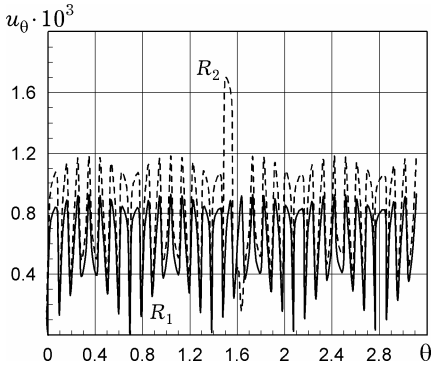

Fig. 3. Dependence of the displacements u_θ at the inner and outer surfaces of the spherical shell on θ.

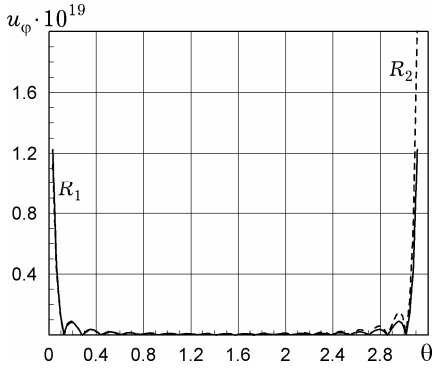

Fig. 4. Dependence of the displacements u_φ at the inner and outer surfaces of the spherical shell on θ.

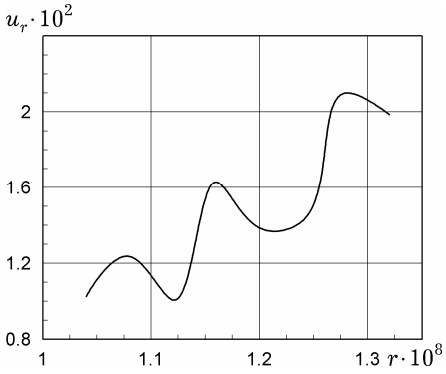

Fig. 5. Dependence of the displacements u_r at the inner and outer surfaces of the spherical shell on r.

In Fig. 4 the same investigation of the displacements u_φ dynamics at the inner and outer surfaces of the spherical shell regarding θ is shown. One can sure that the displacements u_φ values are negligibly less than the values of the displacements u_r and u_θ. In Fig. 5 the dependence of the displacements u_r on radius-vector r at the inner and outer surfaces of the spherical shell is presented. The displacements u_r values increase in the direction from the inner virus surface ($r = R_1$) to the outer surface ($r = R_2$). As can be seen from the figures, the change in the load depending on angle φ is negligible. So one can observe more simple axisymmetric problem.

Conclusions. The 3D idealized virus capsid PCV2 model of a virus was constructed with the help of apparatus of the boundary value problems of dynamic elasticity.

The formulas determining the virus wave field under the acoustic pressure wave were obtained. The graphics of the spherical shell displacements are presented.

This model will serve as a first step in developing more realistic models of viruses with a varying density of the capsid and its thickness.

Appendix A.

$$u_n^i(r,\theta) = \frac{1}{b^2}\sum_{k=|n|}^{\infty}\Bigg[\left(b^2R_i^2 - 2k(k+1)\right)\left\langle u_{nk}^i(R_i)\right\rangle\frac{\partial}{\partial r}\Gamma_{a,k}(r,R_i) +$$

$$+\left(4\left\langle u_{nk}^i(R_i)\right\rangle + \frac{R_i}{\mu}\left\langle \sigma_{rnk}^i(R_i)\right\rangle\right)\frac{\partial^2}{\partial r\partial R_i}\Gamma_{a,k}(r,R_i)\Bigg]\sigma_{k,|n|}P_k^{|n|}(\cos\theta) +$$

$$+\frac{1}{r}\frac{n^2}{\sin^2\theta}\sum_{k=|n|}^{\infty}\frac{R_i}{b^2}\Bigg[\left(2\left\langle u_{nk}^i(R_i)\right\rangle + \frac{R_i}{\mu}\left\langle \sigma_{rnk}^i(R_i)\right\rangle\right)\Gamma_{b,k}(r,R_i) -$$

$$-2\left\langle u_{nk}^i(R_i)\right\rangle\frac{\partial}{\partial R_i}\Gamma_{b,k}(r,R_i)\Bigg]\sigma_{k,|n|}P_k^{|n|}(\cos\theta) -$$

$$-\frac{1}{r}\sum_{k=|n|}^{\infty}\frac{R_i}{b^2}\Bigg[\left(2\left\langle u_{nk}^i(R_i)\right\rangle + \frac{R_i}{\mu}\left\langle \sigma_{rnk}^i(R_i)\right\rangle\right)\Gamma_{b,k}(r,R_i) -$$

$$-2\left\langle u_{nk}^i(R_i)\right\rangle\frac{\partial}{\partial R_i}\Gamma_{b,k}(r,R_i)\Bigg]\sigma_{k,|n|}\frac{d^2}{d\theta^2}P_k^{|n|}(\cos\theta) -$$

$$-\frac{1}{r}\operatorname{ctg}\theta\sum_{k=|n|}^{\infty}\frac{R_i}{b^2}\Bigg[\left(2\left\langle u_{nk}^i(R_i)\right\rangle + \frac{R_i}{\mu}\left\langle \sigma_{rnk}^i(R_i)\right\rangle\right)\Gamma_{b,k}(r,R_i) -$$

$$-2\left\langle u_{nk}^i(R_i)\right\rangle\frac{\partial}{\partial R_i}\Gamma_{b,k}(r,R_i)\Bigg]\sigma_{k,|n|}\frac{d}{d\theta}P_k^{|n|}(\cos\theta)\,,$$

$$v_n^i(r,\theta) = \frac{1}{r}\frac{1}{b^2}\sum_{k=|n|}^{\infty}\Bigg[\left(b^2R_i^2 - 2k(k+1)\right)\left\langle u_{nk}^i(R_i)\right\rangle\Gamma_{a,k}(r,R_i) +$$

$$+\left(4\left\langle u_{nk}^i(R_i)\right\rangle\frac{R_i}{\mu}\left\langle \sigma_{rnk}^i(R_i)\right\rangle\right)\frac{\partial}{\partial R_i}\Gamma_{a,k}(r,R_i)\Bigg]\sigma_{k,|n|}\frac{d}{d\theta}P_k^{|n|}(\cos\theta) +$$

$$+\frac{1}{r}\sum_{k=|n|}^{\infty}\frac{R_i}{b^2}\Bigg[\left(2\left\langle u_{nk}^i(R_i)\right\rangle + \frac{R_i}{\mu}\left\langle \sigma_{rnk}^i(R_i)\right\rangle\right)\Gamma_{b,k}(r,R_i) -$$

$$-2\left\langle u_{nk}^i(R_i)\right\rangle\frac{\partial}{\partial R_i}\Gamma_{b,k}(r,R_i)\Bigg]\sigma_{k,|n|}\frac{d}{d\theta}P_k^{|n|}(\cos\theta) +$$

$$+\sum_{k=|n|}^{\infty}\frac{R_i}{b^2}\Bigg[\left(2\left\langle u_{nk}^i(R_i)\right\rangle + \frac{R_i}{\mu}\left\langle \sigma_{rnk}^i(R_i)\right\rangle\right)\frac{\partial}{\partial r}\Gamma_{b,k}(r,R_i) -$$

$$-2\left\langle u_{nk}^i(R_i)\right\rangle\frac{\partial^2}{\partial r\partial R_i}\Gamma_{b,k}(r,R_i)\Bigg]\sigma_{k,|n|}\frac{d}{d\theta}P_k^{|n|}(\cos\theta)\,,$$

$$w_n^i(r,\theta) = -\frac{in}{r\sin\theta}\frac{1}{b^2}\sum_{k=|n|}^{\infty}\Bigg[\left(b^2R_i^2 - 2k(k+1)\right)\left\langle u_{nk}^i(R_i)\right\rangle\Gamma_{a,k}(r,R_i) +$$

$$+\left(4\left\langle u_{nk}^i(R_i)\right\rangle + \frac{R_i}{\mu}\left\langle \sigma_{rnk}^i(R_i)\right\rangle\right)\frac{\partial}{\partial R_i}\Gamma_{a,k}(r,R_i)\Bigg]\sigma_{k,|n|}P_k^{|n|}(\cos\theta) -$$

$$-\frac{in}{r\sin\theta}\sum_{k=|n|}^{\infty}\frac{R_i}{b^2}\Bigg[\left(2\left\langle u_{nk}^i(R_i)\right\rangle + \frac{R_i}{\mu}\left\langle \sigma_{rnk}^i(R_i)\right\rangle\right)\Gamma_{b,k}(r,R_i) -$$

$$-2\left\langle u_{nk}^i(R_i)\right\rangle\frac{\partial}{\partial R_i}\Gamma_{b,k}(r,R_i)\Bigg]\sigma_{k,|n|}P_k^{|n|}(\cos\theta) -$$

$$-\frac{in}{\sin\theta}\sum_{k=|n|}^{\infty}\frac{R_i}{b^2}\Bigg[\left(2\left\langle u_{nk}^i(R_i)\right\rangle k(k+1) + \frac{R_i}{\mu}\left\langle \sigma_{rnk}^i(R_i)\right\rangle\right)\frac{\partial}{\partial r}\Gamma_{b,k}(r,R_i) -$$

$$- 2\left\langle u^i_{nk}(R_i)\right\rangle \frac{\partial^2}{\partial r \partial R_i}\Gamma_{b,k}(r,R_i)\Big]\sigma_{k,|n|}P_k^{|n|}(\cos\theta)\,,$$

$$\frac{\sigma^i_{rsn}(r,\theta)}{2\mu} = \frac{1}{b^2}\sum_{k=|n|}^{\infty}\Big[\left(b^2R_i^2 - 2k(k+1)\right)\left\langle u^i_{nk}(R_i)\right\rangle \frac{\partial^2}{\partial r^2}\Gamma_{a,k}(r,R_i) +$$

$$+\left(4\left\langle u^i_{nk}(R_i)\right\rangle + \frac{R_i}{\mu}\left\langle \sigma^i_{rnk}(R_i)\right\rangle\right)\frac{\partial^3}{\partial r^2\partial R_i}\Gamma_{a,k}(r,R_i)\Big]\sigma_{k,|n|}P_k^{|n|}(\cos\theta) -$$

$$-\frac{\lambda a^2}{2\mu}\frac{1}{b^2}\sum_{k=|n|}^{\infty}\Big[\left(b^2R_i^2 - 2k(k+1)\right)\left\langle u^i_{nk}(R_i)\right\rangle \Gamma_{b,k}(r,R_i) +$$

$$+\left(4\left\langle u^i_{nk}(R_i)\right\rangle + \frac{R_i}{\mu}\left\langle \sigma^i_{rnk}(R_i)\right\rangle\right)\frac{\partial}{\partial R_i}\Gamma_{b,k}(r,R_i)\Big]\sigma_{k,|n|}P_k^{|n|}(\cos\theta) +$$

$$+ b^2\sum_{k=|n|}^{\infty}\frac{R_i}{b^2}\Big[\left(2\left\langle u^i_{nk}(R_i)\right\rangle + \frac{R_i}{\mu}\left\langle \sigma^i_{rnk}(R_i)\right\rangle\right)\Gamma_{b,k}(r,R_i) -$$

$$- 2\left\langle u^i_{nk}(R_i)\right\rangle \frac{\partial}{\partial R_i}\Gamma_{b,k}(r,R_i)\Big]\sigma_{k,|n|}P_k^{|n|}(\cos\theta) +$$

$$+ b^2 r\sum_{k=|n|}^{\infty}\frac{R_i}{b^2}\Big[\left(2\left\langle u^i_{nk}(R_i)\right\rangle + \frac{R_i}{\mu}\left\langle \sigma^i_{rnk}(R_i)\right\rangle\right)\frac{\partial}{\partial r}\Gamma_{b,k}(r,R_i) -$$

$$- 2\left\langle u^i_{nk}(R_i)\right\rangle \frac{\partial^2}{\partial r\partial R_i}\Gamma_{b,k}(r,R_i)\Big]\sigma_{k,|n|}P_k^{|n|}(\cos\theta) +$$

$$+ 3\sum_{k=|n|}^{\infty}\frac{R_i}{b^2}\Big[\left(2\left\langle u^i_{nk}(R_i)\right\rangle + \frac{R_i}{\mu}\left\langle \sigma^i_{rnk}(R_i)\right\rangle\right)\frac{\partial^2}{\partial r^2}\Gamma_{b,k}(r,R_i) -$$

$$- 2\left\langle u^i_{nk}(R_i)\right\rangle \frac{\partial^3}{\partial r^2\partial R_i}\Gamma_{b,k}(r,R_i)\Big]\sigma_{k,|n|}P_k^{|n|}(\cos\theta) +$$

$$+ r\sum_{k=|n|}^{\infty}\frac{R_i}{b^2}\Big[\left(2\left\langle u^i_{nk}(R_i)\right\rangle + \frac{R_i}{\mu}\left\langle \sigma^i_{rnk}(R_i)\right\rangle\right)\frac{\partial^3}{\partial r^3}\Gamma_{b,k}(r,R_i) -$$

$$- 2\left\langle u^i_{nk}(R_i)\right\rangle \frac{\partial^4}{\partial r^3\partial R_i}\Gamma_{b,k}(r,R_i)\Big]\sigma_{k,|n|}P_k^{|n|}(\cos\theta)\,,$$

$$\frac{\tau^i_{r\theta n}(r,\theta)}{2\mu} = \frac{1}{r}\frac{1}{b^2}\sum_{k=|n|}^{\infty}\Big[\left(b^2R_i^2 - 2k(k+1)\right)\left\langle u^i_{nk}(R_i)\right\rangle \frac{\partial}{\partial r}\Gamma_{a,k}(r,R_i) +$$

$$+\left(4\left\langle u^i_{nk}(R_i)\right\rangle + \frac{R_i}{\mu}\left\langle \sigma^i_{rnk}(R_i)\right\rangle\right)\frac{\partial^2}{\partial r\partial R_i}\Gamma_{a,k}(r,R_i)\Big]\sigma_{k,|n|}\frac{d}{d\theta}P_k^{|n|}(\cos\theta) -$$

$$-\frac{1}{r^2}\frac{1}{b^2}\sum_{k=|n|}^{\infty}\Big[\left(b^2R_i^2 - 2k(k+1)\right)\left\langle u^i_{nk}(R_i)\right\rangle \Gamma_{b,k}(r,R_i) +$$

$$+\left(4\left\langle u^i_{nk}(R_i)\right\rangle + \frac{R_i}{\mu}\left\langle \sigma^i_{rnk}(R_i)\right\rangle\right)\frac{\partial}{\partial R_i}\Gamma_{b,k}(r,R_i)\Big]\sigma_{k,|n|}\frac{d}{d\theta}P_k^{|n|}(\cos\theta) +$$

$$+\sum_{k=|n|}^{\infty}\frac{R_i}{b^2}\Big[\left(2\left\langle u^i_{nk}(R_i)\right\rangle + \frac{R_i}{\mu}\left\langle \sigma^i_{rnk}(R_i)\right\rangle\right)\frac{\partial^2}{\partial r^2}\Gamma_{b,k}(r,R_i) -$$

$$- 2\left\langle u^i_{nk}(R_i)\right\rangle \frac{\partial^3}{\partial r^2\partial R_i}\Gamma_{b,k}(r,R_i)\Big]\sigma_{k,|n|}\frac{d}{d\theta}P_k^{|n|}(\cos\theta) +$$

$$+\frac{1}{r}\sum_{k=|n|}^{\infty}\frac{R_i}{b^2}\Big[\Big(2\big\langle u^i_{nk}(R_i)\big\rangle+\frac{R_i}{\mu}\big\langle\sigma^i_{rnk}(R_i)\big\rangle\Big)\frac{\partial}{\partial r}\Gamma_{b,k}(r,R_i)-$$

$$-2\big\langle u^i_{nk}(R_i)\big\rangle\frac{\partial^2}{\partial r\partial R_i}\Gamma_{b,k}(r,R_i)\Big]\sigma_{k,|n|}\frac{d}{d\theta}P_k^{|n|}(\cos\theta)+$$

$$+\Big(\frac{b^2}{2}-\frac{1}{r^2}\Big)\sum_{k=|n|}^{\infty}\frac{R_i}{b^2}\Big[\Big(2\big\langle u^i_{nk}(R_i)\big\rangle+\frac{R_i}{\mu}\big\langle\sigma^i_{rnk}(R_i)\big\rangle\Big)\Gamma_{b,k}(r,R_i)-$$

$$-2\big\langle u^i_{nk}(R_i)\big\rangle\frac{\partial}{\partial R_i}\Gamma_{b,k}(r,R_i)\Big]\sigma_{k,|n|}\frac{d}{d\theta}P_k^{|n|}(\cos\theta),$$

$$-\frac{\tau^i_{r\varphi n}(r,\theta)}{2\mu}=\frac{in}{r\sin\theta}\frac{1}{b^2}\sum_{k=|n|}^{\infty}\Big[\big(b^2R_i^2-2k(k+1)\big)\big\langle u^i_{nk}(R_i)\big\rangle\frac{\partial}{\partial r}\Gamma_{a,k}(r,R_i)+$$

$$+\Big(4\big\langle u^i_{nk}(R_i)\big\rangle+\frac{R_i}{\mu}\big\langle\sigma^i_{rnk}(R_i)\big\rangle\Big)\frac{\partial^2}{\partial r\partial R_i}\Gamma_{a,k}(r,R_i)\Big]\sigma_{k,|n|}P_k^{|n|}(\cos\theta)-$$

$$-\frac{in}{r\sin\theta}\frac{1}{r}\frac{1}{b^2}\sum_{k=|n|}^{\infty}\Big[\big(b^2R_i^2-2k(k+1)\big)\big\langle u^i_{nk}(R_i)\big\rangle\Gamma_{b,k}(r,R_i)+$$

$$+\Big(4\big\langle u^i_{nk}(R_i)\big\rangle+\frac{R_i}{\mu}\big\langle\sigma^i_{rnk}(R_i)\big\rangle\Big)\frac{\partial}{\partial R_i}\Gamma_{b,k}(r,R_i)\Big]\sigma_{k,|n|}P_k^{|n|}(\cos\theta)-$$

$$+\frac{in}{\sin\theta}\sum_{k=|n|}^{\infty}\frac{R_i}{b^2}\Big[\Big(2\big\langle u^i_{nk}(R_i)\big\rangle+\frac{R_i}{\mu}\big\langle\sigma^i_{rnk}(R_i)\big\rangle\Big)\frac{\partial}{\partial r}\Gamma_{b,k}(r,R_i)-$$

$$-2\big\langle u^i_{nk}(R_i)\big\rangle\frac{\partial^2}{\partial r\partial R_i}\Gamma_{b,k}(r,R_i)\Big]\sigma_{k,|n|}P_k^{|n|}(\cos\theta)+$$

$$+\frac{in}{\sin\theta}\Big(\frac{b^2}{2}-\frac{1}{r^2}\Big)\sum_{k=|n|}^{\infty}\frac{R_i}{b^2}\Big[\Big(2\big\langle u^i_{nk}(R_i)\big\rangle+\frac{R_i}{\mu}\big\langle\sigma^i_{rnk}(R_i)\big\rangle\Big)\Gamma_{b,k}(r,R_i)-$$

$$-2\big\langle u^i_{nk}(R_i)\big\rangle\frac{\partial}{\partial R_i}\Gamma_{b,k}(r,R_i)\Big]\sigma_{k,|n|}P_k^{|n|}(\cos\theta).$$

Here

$$\Gamma_{i,k}(r,R_j)=\frac{\pi i}{2\sqrt{rR_j}}\begin{cases}I_\nu(R_jq_i)K_\nu(rq_i), & r>R_j,\\ I_\nu(rq_i)K_\nu(R_jq_i), & r<R_j,\end{cases}\quad k=0,1,2,\ldots,\ \nu=k+1/2,$$

$q\in\{a,b\}$, $f_{nk}(r)$ is the Fourier – Legendre transform.

1. *Вайсфельд Н. Д., Попов Г. Я.* Нестационарные динамические задачи концентрации упругих напряжений возле сферического дефекта // Изв. РАН. Механика твердого тела. – 2002. – № 3. – С. 90–102.
   Vaisfel'd N. D., Popov G. Ya. Nonstationary dynamic problems of elastic stress concentration near a spherical imperfection // Mech. Solids. – 2002. – **37**, No. 3. – P. 77–88.
2. *Горечко Н. О., Кушнір Р. М.* Термопружний стан складеної пластинки з теплообміном за дії рівномірно розподіленого джерела тепла // Мат. методи та фіз.-мех. поля. – 2011. – **54**, № 1. – С. 153–162.
   Horechko N. O., Kushnir R. M. Thermostressed state of a composite plate with heat exchange under the action of a uniformly distributed heat source // J. Math. Sci. – 2012. – **183**, No. 2. – P. 177–189.
   https://doi.org/10.1007/s10958-012-0805-4.
3. *Гринченко В. Т., Мелешко В. В.* Гармонические колебания и волны в упругих телах. – Киев: Наук. думка, 1981. – 284 с.

4. *Гузь А. Н., Кубенко В. Д.* Теория нестационарной аэрогидроупругости оболочек. – Киев: Наук. думка, 1982. – 400 с. – Методы расчета оболочек: В 5 т. / Под общ. ред. А. Н. Гузя. – Т. 5.
5. *Кіт Г. С., Галазюк В. А.* Осесиметричний напружено-деформований стан тіла з тонким жорстким дисковим теплонепроникним включенням // Мат. методи та фіз.-мех. поля. – 2013. – **56,** № 3. – С. 95–109.
   Kit H. S., Halazyuk V. A. Axisymmetric stress-strain state of a body with thin rigid disk-shaped heat-resistant inclusion // J. Math. Sci. – 2015. – **205**, No. 4. – P. 602–620. – https://doi.org/10.1007/s10958-015-2269-9.
6. *Медведский А. Л.* Динамика неоднородной трансверсально-изотропной сферы в акустической среде // Вестн. Моск. авиац. ин-та. – 2010. – **17**, № 1. – С. 181–186.
7. *Назарчук З. Т., Куриляк Д. Б., Войтко М. В., Кулинич Я. П.* Про взаємодію пружної *SH*-хвилі з міжфазною тріщиною в абсолютно жорсткому з'єднанні пластини з півпростором // Мат. методи та фіз.-мех. поля. – 2012. – **55,** № 2. – С. 107–118.
   Nazarchuk Z. T., Kuryliak D. B., Voytko M. V., Kulynych Ya. P. On the interaction of an elastic SH-wave with an interface crack in the perfectly rigid joint of a plate with a half-space // J. Math. Sci. – 2013. – **192**, No. 6. – P. 609–622. https://doi.org/10.1007/s10958-013-1420-8.
8. *Панасюк В. В., Саврук М. П.* До питання про визначення концентрації напружень у розтягнутій пластині з двома отворами // Мат. методи та фіз.-мех. поля. – 2008. – **51,** № 2. – С. 112–123.
   Panasyuk V. V., Savruk M. P. On the determination of stress concentration in a stretched plate with two holes // J. Math. Sci. – 2009. – **162**, No. 1. – P. 132–148. – https://doi.org/10.1007/s10958-009-9626-5.
9. *Улитко А. Ф.* Напряженное состояние полой сферы, нагруженной сосредоточенными силами // Прикл. механика. – 1968. – **4**, № 5. – С. 38–45.
   Ulitko A. F. Stress state of a hollow sphere loaded by concentrated forces // Int. Appl. Mech. – 1968. – **4**, No. 5. – P. 25–29. https://doi.org/10.1007/BF00886782.
10. *Хай М. В., Грилицький М. Д.* Математичне формулювання граничних умов у задачах тривимірного деформування пластин // Мат. методи та фіз.-мех. поля. – 1999. – **42,** № 1. – С. 55–61.
    Khai M. V., Hrylyts'kyi M. D. Mathematical statement of boundary conditions for problems of three-dimensional deformation of plates // J. Math. Sci. – 2002. – **109**, No. 1. – P. 1221–1228. https://doi.org/10.1023/A:1013744627572.
11. *Хашеминеджад С. М., Малеки М.* Резонансное рассеяние звука погруженной анизотропной сферой // Акуст. журн. – 2008. – 54, № 2. – С. 205–218.
    Hasheminejad S. M., Maleki M. Acoustic resonance scattering from a submerged anisotropic sphere // Acoust. Phys. – 2008. – **54**, No. 2. – P. 168–179. https://doi.org/10.1134/S1063771008020048.
12. *Чернина В. С.* Статика тонкостенных оболочек вращения. – Москва: Наука, 1968. – 456 с.
13. *Шептилевский А. В., Косенков В. М., Селезов И. Т.* Трёхмерная модель гидроупругой системы, ограниченной сферической оболочкой // Мат. методи та фіз.-мех. поля. – 2012. – **55,** № 1. – С. 159–167.
    Sheptilevskiy A. V., Kosenkov V. M., Selezov I. T. Three-dimensional model of a hydroelastic system bounded by a spherical shell // J. Math. Sci. – 2013. – **190**, No. 6. – P. 823–834. https://doi.org/10.1007/s10958-013-1291-z.
14. *Aglyamov S. R., Karpiouk A. B., Ilinskii Yu. A., Zabolotskaya E. A., Emelianov S. Y.* Motion of a solid sphere in a viscoelastic medium in response to applied acoustic radiation force: Theoretical analysis and experimental verification // J. Acoust. Soc. Am. – 2007. – **122**, No. 4. – P. 1927–1936. https://doi.org/10.1121/1.2774754.
15. *Buenemann M., Lenz P.* Elastic properties and mechanical stability of chiral and filled viral capsids // Phys. Rev. **E**. – 2008. – **78**, No. 5. https://doi.org/10.1103/PhysRevE.78.051924.
16. *Buenemann M., Lenz P.* Mechanical limits of viral capsids // Proc. Natl. Acad. Sci. USA (PNAS). – 2007. – **104**, No. 24. – P. 9925–9930. https://doi.org/10.1073/pnas.0611472104.

17. *Carrasco C., Carreira A., Schaap I. A. T., Serena P. A., Gómez-Herrero J., Mateu M. G., de Pablo P. J.* DNA-mediated anisotropic mechanical reinforcement of a virus // Proc. Natl. Acad. Sci. USA (PNAS). – 2006. – **103**, No. 37. – P. 13706–13711. – https://doi.org/10.1073/pnas.0601881103.
18. *Gibbons M. M., Klug W. S.* Nonlinear finite-element analysis of nanoindentation of viral capsids // Phys. Rev. **E**. – 2007. – **75**, No. 3. https://doi.org/10.1103/PhysRevE.75.031901.
19. *Grason G. M.* Perspective: Geometrically frustrated assemblies // J. Chem. Phys. – 2016. – **145**. – P. 110901-1–110901-17. – https://doi.org/10.1063/1.4962629.
20. *Kiselyova N. N., Shushkevich G. Ch.* Acoustic scattering by spherical shell and sphere // Computer Algebra Systems in Teaching and Research: Mathematical Modeling in Physics, Civil Engineering, Economics and Finance. – Siedlce: Wydawnictwo Collegium Mazovia, 2011. – P. 91–99. https://elib.grsu.by/katalog/161816-348205.pdf.
21. *Korotkin I., Nerukh D., Tarasova E., Farafonov V., Karabasov S.* Two-phase flow analogy as an effective boundary condition for modelling liquids at atomistic resolution // J. Comput. Sci. – 2016. – **17**, part 2. – P. 446–456. https://doi.org/10.1016/j.jocs.2016.03.012.
22. *Lidmar J., Mirny L., Nelson D. R.* Virus shapes and buckling transitions in spherical shells // Phys. Rev. **E**. – 2003. – **68**, No. 5. https://doi.org/10.1103/PhysRevE.68.051910.
23. *Markesteijn A., Karabasov S., Scukins A., Nerukh D., Glotov V., Goloviznin V.* Concurrent multiscale modelling of atomistic and hydrodynamic processes in liquids // Phil. Trans. R. Soc. **A**. Math. Phys. Eng. Sci. – 2014. – **372**, No. 2021. doi: 10.1098/rsta.2013.0379.
24. *May E. R., Brooks C. L.* (*3rd*) On the morphology of viral capsids: Elastic properties and buckling transitions // J. Phys. Chem. **B**. – 2012. – **116**, No. 29. – P. 8604–8609. – DOI:10.1021/jp300005g.
25. *Mykhas'kiv V. V., Zhbadynskyi I. Ya., Zhang Ch.* Dynamic stresses due to time-harmonic elastic wave incidence on doubly periodic array of penny-shaped cracks // Мат. методи та фіз.-мех. поля. – 2013. – **56**, № 2. – С. 94–101.
Те саме: *Mykhas'kiv V. V., Zhbadynskyi I. Ya., Zhang Ch.* Dynamic stresses due to time-harmonic elastic wave incidence on doubly periodic array of penny-shaped cracks // J. Math. Sci. – 2014. – **203**, No. 1. – P. 114–122. https://doi.org/10.1007/s10958-014-2094-6.
26. *Nowacki W.* Teoria sprężystości. – Warszawa: Państwowe Wydawnictwo Naukowe, 1970. – 770 s.
Новацкий В. Теория упругости. – Москва: Мир, 1975. – 872 с.
27. *Phillips R., Dittrich M., Schulten K.* Quasicontinuum representations of atomic-scale mechanics: from proteins to dislocations // Annu. Rev. Mater. Res. – 2002. – **32**. – P. 219–233. https://doi.org/10.1146/annurev.matsci.32.122001.102202.
28. *Polles G., Indelicato G., Potestio R., Cermelli P., Twarock R., Micheletti C.* Mechanical and assembly units of viral capsids identified via quasi-rigid domain decomposition // PLOS Comput. Biol. – 2013. – **9**, No. 11. – e1003331. https://doi.org/10.1371/journal.pcbi.1003331.
29. *Roos W. H., Gibbons M. M., Arkhipov A., Uetrecht C., Watts N. R., Wingfield P. T., Steven A. C., Heck A. J., Schulten K., Klug W. S., Wuite G. J.* Squeezing protein shells: How continuum elastic models, molecular dynamics simulations, and experiments coalesce at the nanoscale // Biophys. J. – 2010. – **99**, No. 4. – P. 1175–1181. https://doi.org/10.1016/j.bpj.2010.05.033.
30. *Scukins A., Nerukh D., Pavlov E., Karabasov S., Markesteijn A.* Multiscale molecular dynamics/hydrodynamics implementation of two dimensional «Mercedes Benz» water model // Eur. Phys. J. Special Topics. – 2015. – **224**, No. 12. – P. 2217–2238. https://dx.doi.org/10.1140/epjst/e2015-02409-8.
31. *Titchmarsh E. C.* Introduction to the theory of Fourier integrals. – Oxford: Oxford Univ. Press, 1948. – viii+394 p.
32. *Vliegenthart G. A., Gompper G.* Mechanical deformation of spherical viruses with icosahedral symmetry // Biophys. J. – 2006. – **91**, No. 3. – P. 834–841. https://doi.org/10.1529/biophysj.106.081422.
33. *Wu J. H., Liu A. Q., Chen H. L., Chen T. N.* Multiple scattering of a spherical acoustic wave from fluid spheres // J. Sound Vib. – 2006. – **290**, No. 1-2. – P. 17–33. https://doi.org/10.1016/j.jsv.2005.03.015.

34. *Zandi R., Reguera D.* Mechanical properties of viral capsids // Phys. Rev. **E**. – 2005. – **72**, No. 2. – https://doi.org/10.1103/PhysRevE.72.021917.
35. *Zhuravlova Z., Kozachkov D., Pliusnov D., Radzivil V., Reut V., Shpynarov O., Tarasova E., Nerukh D., Vaysfel'd N.* Modelling of virus vibration with 3-D dynamic elasticity theory // 23rd Int. Conf. «Engineering mechanics 2017», 15–18 May, 2017, Svratka, Czech Republic, 2017. – P. 1126–1129.
36. *Zink M., Grubmüller H.* Mechanical properties of the icosahedral shell of southern bean mosaic virus: A molecular dynamics study // Biophys. J. – 2009. – **96**, No. 4. – P. 1350–1363. – https://doi.org/10.1016/j.bpj.2008.11.028.

ДОСЛІДЖЕННЯ ІДЕАЛІЗОВАНОЇ МОДЕЛІ ВІРУСУ КАПСИДУ ЗА ДОПОМОГОЮ АПАРАТУ ДИНАМІЧНОЇ ТЕОРІЇ ПРУЖНОСТІ

Тривимірну динамічну теорію пружності застосовано при дослідженні механічних властивостей вірусу капсиду. Ідеалізована модель вірусу базується на тривимірній крайовій задачі математичної фізики, що сформульована у сферичній системі координат для усталених коливань. Вірус моделюється порожнистою пружною сферою, заповненою деяким акустичним середовищем і оточеною іншим акустичним середовищем. Крайову задачу розв'язано за допомогою методу інтегральних перетворень в методу розривних розв'язків. Отримано точний розв'язок задачі. Виконано обчислення пружних характеристик вірусу.

ИССЛЕДОВАНИЕ ИДЕАЛИЗИРОВАННОЙ МОДЕЛИ ВИРУСА КАПСИДА С ПОМОЩЬЮ АППАРАТА ДИНАМИЧЕСКОЙ ТЕОРИИ УПРУГОСТИ

Трёхмерная динамическая теория упругости применена к исследованию механических свойств вируса капсида. Идеализированная модель вируса основана на трёхмерной краевой задаче математической физики, сформулированной в сферической системе координат для установившихся колебаний. Вирус моделируется полой упругой сферой, заполненной некоторой акустической средой, размещенной в другой акустической среде. Краевая задача решена с помощью метода интегральных преобразований и метода разрывных решений. Получено точное решение задачи. Выполнены вычисления упругих характеристик вируса.

[1] Odessa I. I. Mechnikov National University, Odessa,
[2] Aston University, Birmingham, UK

Одержано
19.09.17